International Journal on Interactive Design and Manufacturing (IJIDeM) (2023) 17:869–885
https://doi.org/10.1007/s12008-022-01186-4

ORIGINAL PAPER

Investigation of dimensional accuracy of material extrusion build parts using mathematical modelling and artificial neural network

Ashutosh Kumar Gupta[1] · Mohammad Taufik[1]

Received: 5 July 2022 / Accepted: 25 December 2022 / Published online: 4 January 2023

Abstract

Dimensional accuracy of fabricated parts made through material extrusion process is an important parameter to decide the part's quality. Since a 3D model part is produced in layered form, the deposited layers are subjected to heat for multiple times. Also, deposited layers form bonds with adjacent layers and roads. It leads to shrinkage and distortion in fabricated parts. Process variables are also significant parameters to decide the final part dimension. Accuracy of the parts can be improved if the dimensions are predicted in an earlier stage. So, for the prediction of accurate result various mathematical models have been formulated by the researchers. Use of soft computing techniques can be one method which may also be used for prediction. Since the experiments are performed at various combination of process variables. RSM uses different mathematical models for each set of experiment, but ANN can be use at same parameters. Thus, in this paper ANN model is compared with the developed models of the selected existing literatures. Also, these models are used to find and compare the effect of process variables on dimensional accuracy. The results show that ANN model predicts the results with very less error in comparison of existing models.

Keywords Material extrusion · Modelling · Soft computing · Dimensional accuracy · ANN · Additive manufacturing

1 Introduction

Nowadays, material extrusion additive manufacturing (MEAM) is one of the most used techniques utilized for prototyping, rapid tooling and inhouse fabrication. The MEAM process can be divided into three types: first is fused filament fabrication, second is screw based pellets extrusion (SBPE) and last is plunger-based extrusion process. In these types of MEAM process, FFF and SBPE are most commonly used techniques [1, 2]. Figure 1 (a and b) shows the schematic of FFF and SBPE methods. MEAM techniques are used to fabricate 3D parts by depositing materials layer-by-layer. Mostly, thermoplastic polymers are used as filaments and pellets to produce 3D parts [3].

One of the important quality characteristics in the printed objects using FFF and SBPE is dimensional accuracy. Dimensional accuracy must be studied in FFF and SBPE processes to produce accurate individual parts' dimensions. Since a product consists of several parts which are assembled in the last stage of product finishing. The assembly of the parts needs accurate dimensions because if the fabricated individual parts do not meet specifications, then the problems in assembly may arise. Volumetric or dimensional error is a well-known error in produced parts using MEAM methods. Surface roughness is also a major drawback of MEAM methods.

Various researchers have worked on the improvement of dimensional accuracy of parts fabricated using MEAM processes by considering different process parameters and optimization methods. Also, various authors have studied the effects process variables on the dimensional accuracy of the parts. Very few of them used soft computing techniques to predict the results. Some related works are presented in the next section.

Budzik et al. [5] discussed the strategies for quality enhancement of additively manufactured parts using polymer form materials. On the basis of the state of the process, quality control process is categories in three levels namely quality control during data generation, quality control during manufacturing, quality control during post processing. In this study visual prototype assessment technique was used in

✉ Mohammad Taufik
taufikmohd86@gmail.com

[1] Department of Mechanical Engineering, Maulana Azad National Institute of Technology, Bhopal 462003, India

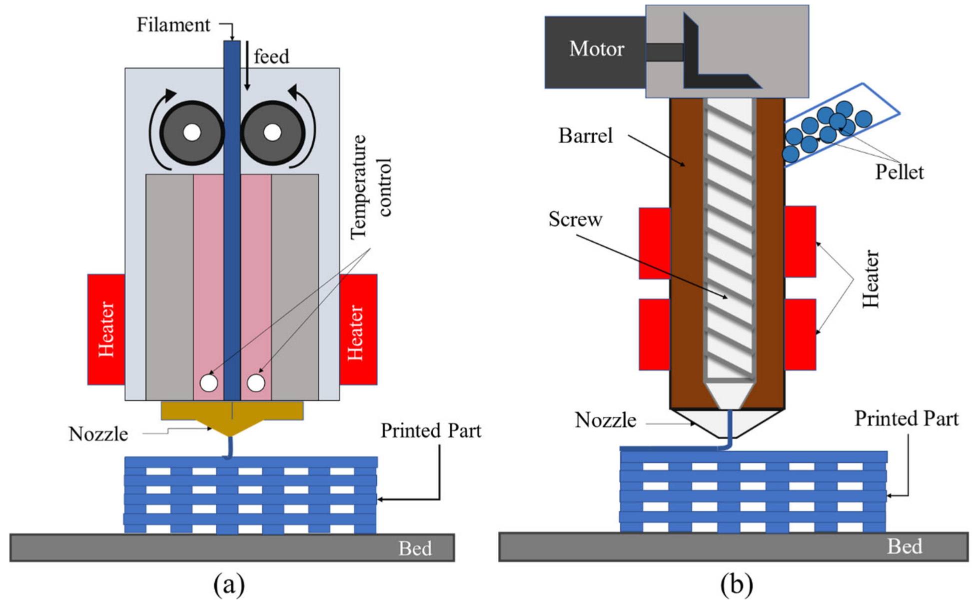

Fig. 1 Schematic of (**a**) fused filament fabrication (**b**) screw-based pellets extrusion [4]

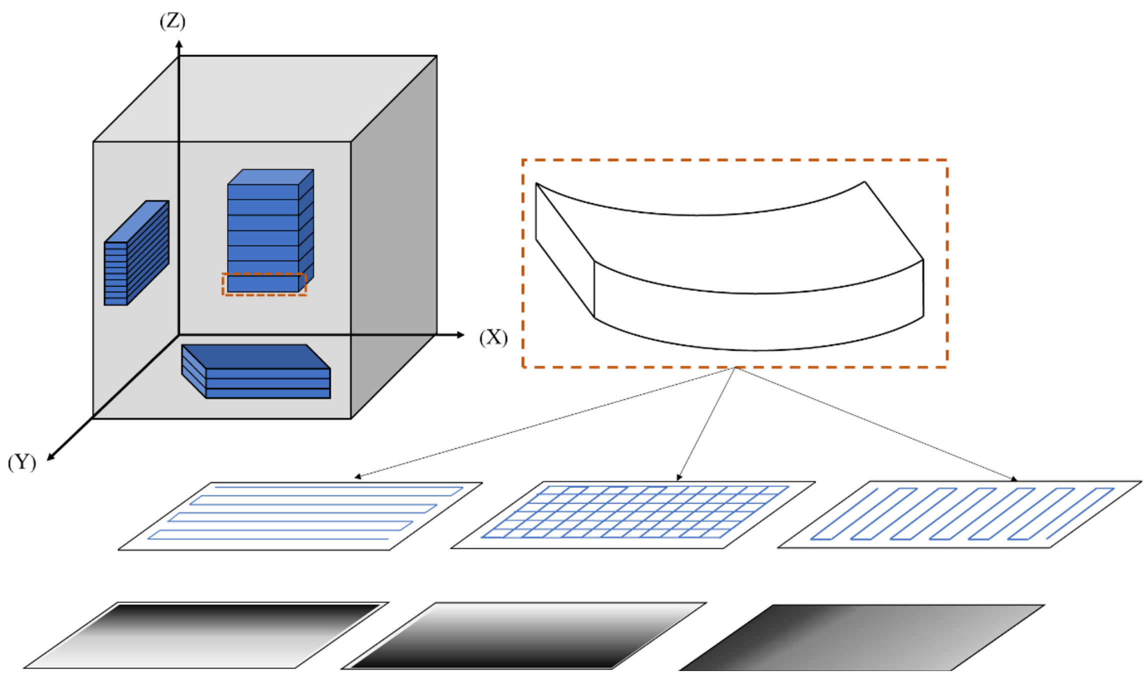

Fig. 2 Variation of stress concentration at different raster patterns

quality control and it was found that the MEM method was less accurate among other processes like FDM, polyjet, DLP, etc. methods. Chen et al. [6] proposed a low-cost approach to characterize the rheological properties in AM. In this study melt flow behavior of polymers and pressure drop in nozzle was computed. Nieto et al. [7] presented a case study to develop a prototype of a large format pellet-based AM system to extrude the polymers for industrial use. The polymers PLA and ABS were selected to extrude and fabricate layered parts. Masood et al. [8] formulated a mathematical model that can be suitable to compute the volumetric error for any build orientation. This model was applied to various shapes (like cylinder, cube, pyramid, and sphere) and the calculated error of these shapes was compared with the experimental results. The accuracy of the developed model was significant, and the authors concluded that this mathematical model can be further extended to calculate the volumetric error of complex shapes. Garg et al. [9] analyzed the effect of build orientation on the dimensional accuracy and surface roughness of parts printed using FDM process. The printed

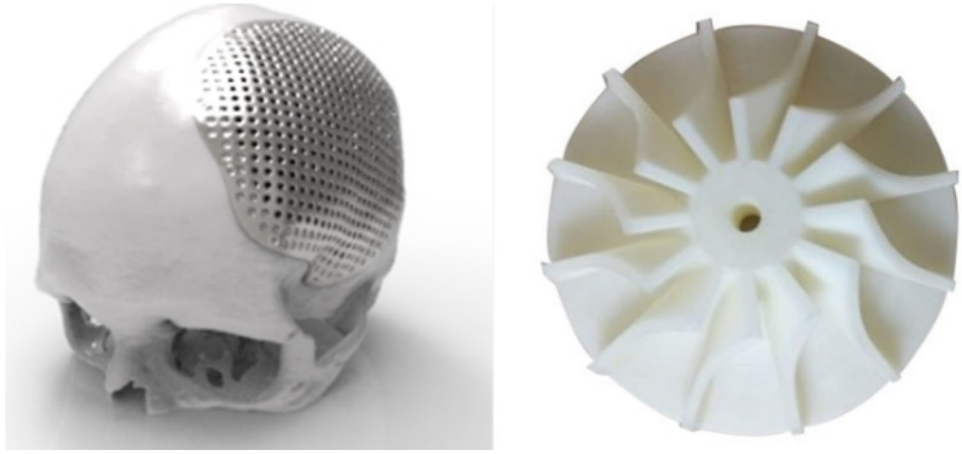

Fig. 3 Practical use of AM in medical and aerospace sectors [14, 15]

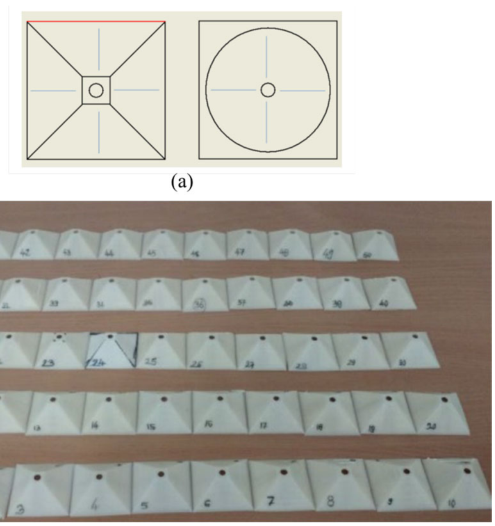

Fig. 4 Test Specimens [17]

parts are also post processed by using cold vapor treatment to enhance the surface finish and dimensional accuracy. Thaisa et al. [10] presented a review study on the use of AM in dental implants. Custom implants like dental implants need microscopic resolution and sufficient bone height and thickness. So, in the individualized implants AM has significant potential to replace older processes if the parts made using AM processes reach up to desired surface finish and dimensional accuracy. Perez et al. [11] studied the surface roughness and dimensional accuracy of FFF fabricated parts. It was found that at lower layer height good surface finish can be achieved but this increases fabrication time. Zhang and Chou [12] investigated the heat and mass transfer phenomena in the FDM process. Figure 2 shows that the effect of the various tool path on the stress concentration directions. In this study simulation was performed at various tool path strategies. It was found that principal stress generated due to heat accumulated at the location of starting point of deposition. At the 90° raster angle bead is deposited along the length. So, long rater patter is obtained which generated the stress concentration at the adjacent previous layer. Since the stress is concentrated at a specific location this can generates the bending and distortion in the parts.

As the material extrusion AM processes are being rapidly used for prototyping and producing medical models. In such applications a very high order of dimensional accuracy is being needed [13]. Figure 3 shows an example of the various practical use where a very high accuracy of the parts is necessary. The dimensional accuracy of the produced models varies for different materials and processes, or technologies used. The accuracy can be enhanced if it is estimated at the earlier stage.

In this work, a unique method using an ANN modelling is developed for the prediction of dimensional accuracy of the parts printed using extrusion based additive manufacturing process. The ANN methodology provides the modelling of complex relationships, spatially non-linear activation functions that can be investigated without complicated expressions. Due to flexibility with the number of experimental data, ANN makes it possible to use more familiar experimental designs. Also, ANN models may have better prediction power then regression models. So, the purpose of this work is to predict the accuracy of printed parts by using a soft computing technique (artificial neural network). Also, the mathematical models used by the authors in their literature are compared with the ANN models for the prediction of accuracy of printed parts. Thus, this research shows an integrated approach for part design and manufacturing with the involvement of ANN based computing technique for the modelling and predictive analysis of dimensional accuracy for additively manufactured discrete artefacts.

This paper is organized as follows: Sect. 2 introduces some needful information part design and measurement of dimensional accuracy. Section 3 represents the DoE based

Table 1 Process variables and their level used by various authors

Literature	Process Variables	Levels
Mohamed et al. [16]	Layer height	0.254; 0.178; 0.127
	Orientation	30; 15;0
	Raster angle	60; 30, 0
	Raster width	0.5064; 0.4564; 0.4064
	Air gap	0.008; 0.004; 0
Vyavahare et al. [17]	Barrel temperature	100, 110, 120
	Bed temperature	30, 40, 50
	Build orientation	0, 45, 90
	Raster angle	0, 45, 90
	No. of Contours	1, 2, 3
Jung et al. [18]	Outlet Size	50, 57.32, 75, 93.68, 100
	Hopper angle	30, 37.32, 55, 72.68, 80

mathematical modelling. Section 4 proposes the ANN architecture and modelling. Section 5 discusses the comparison of developed model with existing models, and conclusions are made in Sect. 6.

2 Part design and measurement of dimensional accuracy

In the literature, various techniques have been used by the researcher for the measurement of the dimensional accuracy or percentage error in dimensions of FFF and SBME manufactured parts. Researchers have adopted the various test specimens as per their CAD modelling packages and at the basis of precision of the 3D printer. The CAD model and the fabricated parts are shown in the Fig. 4. Mohamed et al. [16] followed the Eq. 1, Vyavahare et al. [17] followed Eq. 2 to measure the percentage difference of fabricated test specimens. In the Eq. 1, ΔD is the percentage difference in diameter, D_{EXP}, and D_{CAD} are the dimeter of parts fabricated and CAD model file. Jung et al. [18] measured the discharge time. To measure the dimension of the parts Mohamed et al. [16] used Mitutoyo Precision Micrometer (precision of 0.01 mm), Vyavahare et al. [17] used the caliper (gauging range of 0 mm–150 mm and precision of 0.01 mm) and Jung et al. [18] used a high-speed camera with time stamping records to measure the discharge time.

$$\Delta D = \left| \frac{D_{EXP} - D_{CAD}}{\frac{D_{EXP}+D_{CAD}}{2}} \right| \times 100 \tag{1}$$

$$\Delta L(\%) = \frac{Length\ of\ CAD\ model - Length\ of\ fabricated\ model}{Length\ of\ CAD\ model} \times 100 \tag{2}$$

3 DOE based mathematical modelling

Mathematical modelling is the best tool to formulate the relationship between process parameters and the output variables. The response surface methodology (RSM) is one of such as tool that is useful to formulate an analytical model for the targeted output variables. In this work dimensional accuracy (percentage change in various dimensions) and discharge time were selected as the output variables based on the available literatures. Equation 3 shows a generalized full quadratic response surface model used to obtain mathematical relation [16]–[18].

$$y = \beta_0 + \sum_{i=1}^{k} \beta_i X_i + \sum_{i=1}^{k} \beta_{ii} X_i X_i + \sum_{i<j} \sum \beta_{ij} X_i X_j + \varepsilon \tag{3}$$

where y: output function; X_i, X_j: independent variables; β_0: regression constants for intercept; β_i: regression constants for linear term; β_{ii}, and β_{ij}: regression constants for quadratic term.

Researchers can select any of the DOE techniques as per their need and suitability, out of various techniques available in the literature. Box-Behnken, Taguchi orthogonal array, central composite design etc. are the generally used DOE methods. Mohamed et al. [16] used IV-optimal RSM design, Vyavahare et al. [17] implemented the central composite design (CCD) and Jung et al. [18] implemented central composite rotatable design (CCRD) to perform the experiments. Table 1 shows parameters level used by various authors for evaluating the effects on dimensional accuracy of the fabricated parts.

For the description of process parameters and dimensional accuracy, a mathematical relationship between them is required. By formulating an approximate expression, in the fitness problem the response surface methodology has been used in place of controllable factors. Mohamed et al. [16], Vyavahare et al. [17] and Jung et al. [18] applied the least square method for generating the functional expression. The generated functional expressions are shown in Eqs. (2–9). Many authors also evaluate the significance of process parameters and formulated expressions, using the analysis of variance. The ANOVA test is mostly performed using the software such as MINITAB, STATISTICA and Design Expert [16, 17]. The process parameters and expressions are assumed to be significant if the low probability (P-value) is lower than 0.05.

$$
\begin{aligned}
\Delta D(\%) = & -9.52 - 28.18 \times layer\ thickness\ - 0.735 \\
& \times airgap\ - 0.003274 \times raster\ angle \\
& + 0.00376 \times orientation + 51.4 \\
& \times raster\ width - 0.0511 \times No.of\ contours \\
& - 6.675 \times layer\ thickness \times air\ gap \\
& + 0.03629 \times layer\ thickness \\
& \times orientation + 17.39 \times layer\ thickness \\
& \times road\ width + 0.3804 \times layer\ thickness \\
& \times no.of\ contours\ - 0.01486 \times airgap \\
& \times raster\ angle\ - 0.01405 \times airgap \\
& \times orintation\ - 3.4 \times 10^{-5} \times raster\ angle \\
& \times orientation + 58.04 \times layer\ thickness^2 \\
& + 4.861 \times airgap^2 - 5.9 \times 10^{-5} \\
& \times orientation^2 - 53.2 \times no.of\ contours^2
\end{aligned}
\tag{4}
$$

$$
\begin{aligned}
\Delta Length = & \ 115.77 - 58.1 \times Layer\ thickness + 0.051 \\
& \times Print\ speed + 0.029 \times Build\ orientation \\
& + 23.2 \times wall\ thickness\ - 1.029 \\
& \times Extrusion\ temperature + 0.016 \\
& \times Layer\ thickness \times Print\ speed\ - 0.019 \\
& \times Layer\ thickness \times Build\ orientation \\
& - 1.99 \times Layer\ thickness \times wall\ thickness \\
& + 0.068 \times Layer\ thickness \\
& \times Extrusion\ temperature + 0.00002 \\
& \times Print\ speed \times Build\ orientation \\
& + 0.013 \times Print\ speed \times wall\ thickness \\
& - 0.0003 \times Print\ speed \\
& \times Extrusion\ temperature\ - 0.011 \\
& \times Build\ orientation \times wall\ thickness \\
& - 0.00004 \times Build\ orientation \\
& \times Extrusion\ temperature\ - 0.005 \\
& \times wall\ thickness \times Extrusion\ temperature \\
& + 111.13 \times Layer\ thickness^2 \\
& - 0.00002 \times Print\ speed^2 \\
& - 0.00003 \times Build\ orientation^2 \\
& - 9.54 \times wall\ thickness^2 \\
& + 0.0022 \times Extrusion\ temperature^2
\end{aligned}
\tag{5}
$$

$$
\begin{aligned}
\Delta width = & \ 44.16 - 6.061 \times Layerthickness + 0.021 \\
& \times Printspeed + 0.004 \times Buildorientation \\
& + 2.93 \times wallthickness - 0.36 \\
& \times Extrusiontemperature + 0.0019 \\
& \times Layerthickness \times Printspeed - 0.041 \\
& \times Layerthickness \times Buildorientation \\
& - 0.46 \times Layerthickness \times wallthickness \\
& + 0.0013 \times Layerthickness \\
& \times Extrusiontemperature + 1.85E - 06 \\
& \times Printspeed \times Buildorientation + 0.0012 \\
& \times Printspeed \times wallthickness - 0.00009 \\
& \times Printspeed \times Extrusiontemperature \\
& - 0.001 \times Buildorientation \times wallthickness \\
& - 3.47E - 06 \times Buildorientation \\
& \times Extrusiontemperature - 0.016 \\
& \times wallthickness \times Extrusiontemperature \\
& - 8.2 \times Layerthickness^2 \\
& - 0.00001 \times Printspeed^2 - 4.7E \\
& - 06 \times Buildorientation^2 \\
& - 0.36 \times wallthickness^2 \\
& + 0.0007 \times Extrusiontemperature^2
\end{aligned}
\tag{6}
$$

$$
\begin{aligned}
\Delta Height = & -141.06 - 26.23 \times Layer\ thickness + 0.12 \\
& \times Print\ speed + 0.04 \times Build\ orientation \\
& - 31.27 \times wall\ thickness + 1.3 \\
& \times Extrusion\ temperature + 0.05 \\
& \times Layer\ thickness \times Print\ speed\ - 0.013 \\
& \times Layer\ thickness \times Build\ orientation \\
& + 0.26 \times Layer\ thickness \times wall\ thickness \\
& + 0.028 \times Layer\ thickness \\
& \times Extrusion\ temperature + 0.00005 \\
& \times Print\ speed \times Build\ orientation \\
& - 0.02 \times Print\ speed \times wall\ thickness \\
& - 0.0003 \times Print\ speed \\
& \times Extrusion\ temperature\ - 0.0075 \\
& \times Build\ orientation \times wall\ thickness \\
& + 0.00001 \times Build\ orientation
\end{aligned}
$$

$$\begin{aligned}&\times\ Extrusion\,temperature\\&-0.053\ \times\ wall\,thickness\\&\times\ Extrusion\,temperature\\&+32.12\times Layer\,thickness^2\\&-0.0004\times Print\,speed^2\\&-0.0002\times Build\,orientation^2\\&+9.35\times wall\,thickness^2\\&-0.0028\times Extrusion\,temperature^2\end{aligned}\tag{7}$$

$$\begin{aligned}(\Delta diameter)^{0.5} = & -32.14-3.03\times Layer\,thickness\\&-0.005\ \times\ Print\,speed+0.012\\&\times\ Build\,orientation+1.9\\&\times\ wall\,thickness+0.27\\&\times\ Extrusion\,temperature+0.03\\&\times\ Layer\,thickness\ \times\ Print\,speed\\&-0.007\ \times\ Layer\,thickness\\&\times\ Build\,orientation\ -0.89\\&\times\ Layer\,thickness\ \times\ wall\,thickness\\&+0.008\ \times\ Layer\,thickness\\&\times\ Extrusion\,temperature\\&+0.00001\ \times\ Print\,speed\\&\times\ Build\,orientation+0.0009\\&\times\ Print\,speed\ \times\ wall\,thickness\\&+0.00009\ \times\ Print\,speed\\&\times\ Extrusion\,temperature\\&+0.0007\ \times\ Build\,orientation\\&\times\ wall\,thickness\ -0.00004\\&\times\ Build\,orientation\\&\times\ Extrusion\,temperature\\&-0.0334\ \times\ wall\,thickness\\&\times\ Extrusion\,temperature\\&+4.41\times Layer\,thickness^2\\&-0.0002\times Print\,speed^2\\&-0.00002\times Build\,orientation^2\\&+2.8\times wall\,thickness^2\\&-0.0005\times Extrusion\,temperature^2\end{aligned}\tag{8}$$

$$\begin{aligned}y_{case1} = & \ 15.7781-0.2499\times outlet\,size\ -0.0792\\&\times\ hopper\,angle+0.0008\ \times\ outlet\,size\\&\times\ hopper\,angle+0.0011\times outlet\,size^2\\&-0.0001\times hopper\,angle^2\end{aligned}\tag{9}$$

$$\begin{aligned}y_{case2} = & \ 20.1556-0.2499\times\ outlet\,size-0.3163\\&\times\ hopper\,angle-0.1112\times\ outlet\,size\\&\times\ hopper\,angle+0.0013\times outlet\,size^2\\&-0.0001\times hopper\,angle^2\end{aligned}\tag{10}$$

$$\begin{aligned}y_{case3} = & \ 22.4699-0.3785\times\ outlet\,size\ -0.1055\\&\times\ hopper\,angle\ -0.0013\ \times\ outlet\,size\\&\times\ hopper\,angle+0.0016\times outlet\,size^2\\&-0.0002\times hopper\,angle^2\end{aligned}\tag{11}$$

4 Artificial neural network (ANN)

Process time, surface integrity, strength, dimensional accuracy, etc. are the common responses in many of the manufacturing process. The controllable and uncontrollable process parameters affect these responses [19]. Hence, to achieve the desired response, the process parameters are required to be required. To handle large amount of data generated from process monitoring, failure mechanisms, and experimental data necessitates the implementation of artificial intelligence (AI). The Large data are better handled by ANN algorithms [20][21].

There are some basic terms in ANN, such as number of layers, and various functions such as activation function and loss function. A typical neural network contains mainly three layers that are named as input layer, hidden layer, and output layer. Out of these three layers, neurons from hidden can only be altered. From the literature [23] it has been observed that one hidden layer with 5–10 neurons shows a better performance with lesser iteration time. The work of activation function is to determine the transformation of weighted some of inputs into an output through the nodes of the ANN network. Binary step, linear, and non-linear are the main three activation function. In these activation functions only, non-linear functions can be used for backpropagation because the derivative functions are related to the inputs. Further, non-linear activation function can be classified into ten various types. Most commonly used linear and non-linear activation functions are tansig, logsig, and purelin. Tansig function is also commonly known as hyperbolic tangent function. In tansig function, the output is 'Zero' centered, hence it indicates the output values to be highly negative, neutral, or highly positive. Logsig (sigmoid) is also known as logistic activation function. Sigmoid function accepts any real number as an input and output is in the range of 0 to 1. As the figure shown in Table 2 corresponding to logsig, it can be observed that this function returns one for larger number input and

Table 2 Activation functions used in ANN

Tansig	$Z(x) = \frac{2}{1+e^{-x}} - 1$	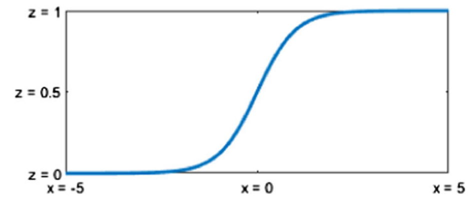
Logsig	$Z(x) = \frac{1}{1+e^{-x}}$	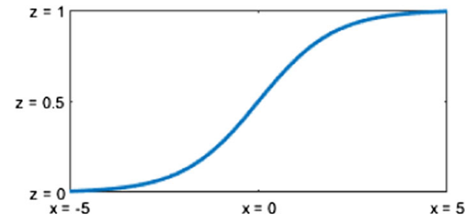
Purelin	$Z(x) = x$	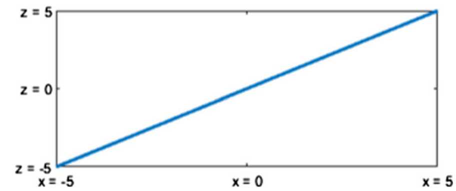

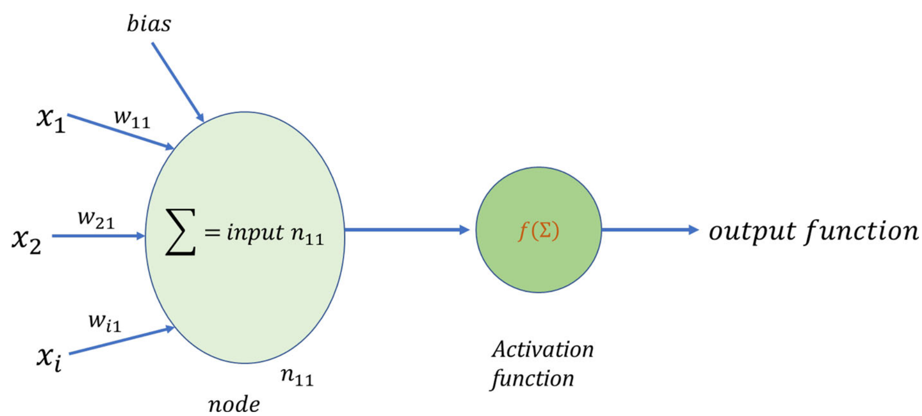

Fig. 5 Schematic of an ANN architecture [22]

zero for smaller value inputs. It is mostly used for the models where probability prediction used as an output. Purelin function is a type of linear activation function. A schematic of the weighted sum in the neural network has been illustrated in Fig. 5. In the Eq. 10: 'i' is number of input (or process variables), 'j' is no. of neurons in hidden layer, 'k' is training cases, 'g' is the activation function, some frequently used activation functions are given in Table 2, 'w' and 'B' is weight assigned to each input neurons and bias respectively.

$$F_{jk} = g\left(\sum(w_{ji}x_{ik}) + B_j\right) \tag{12}$$

In this study the optimum ANN model has been generated by implementing a trial and error method for deciding the number of hidden layer neurons. Each ANN architecture is trained at least three times for to get minimum MSE and maximum R value. The developed model considered feed forward BPNN algorithm with the single hidden layer. As depicted In the Fig. 6, a correlation has been formulated between the experimental and predicted values has been developed for three sets (i.e., training, validation, test). Figure 6 also shows the overall performance of the optimal ANN structure. The R value for response (i.e., percentage error in dimension) for the literature Mohamed et al. [16] is 0.98072. The R value for percentage error in length, width, diameter, and height for the literature Vyavahare et al. [17] are 0.94918, 0.97395, 0.87413 and 0.90175 respectively. The R value for response (i.e., discharge time for all cases) for the literature are 0.99924, 0.99977 and 0.99758.

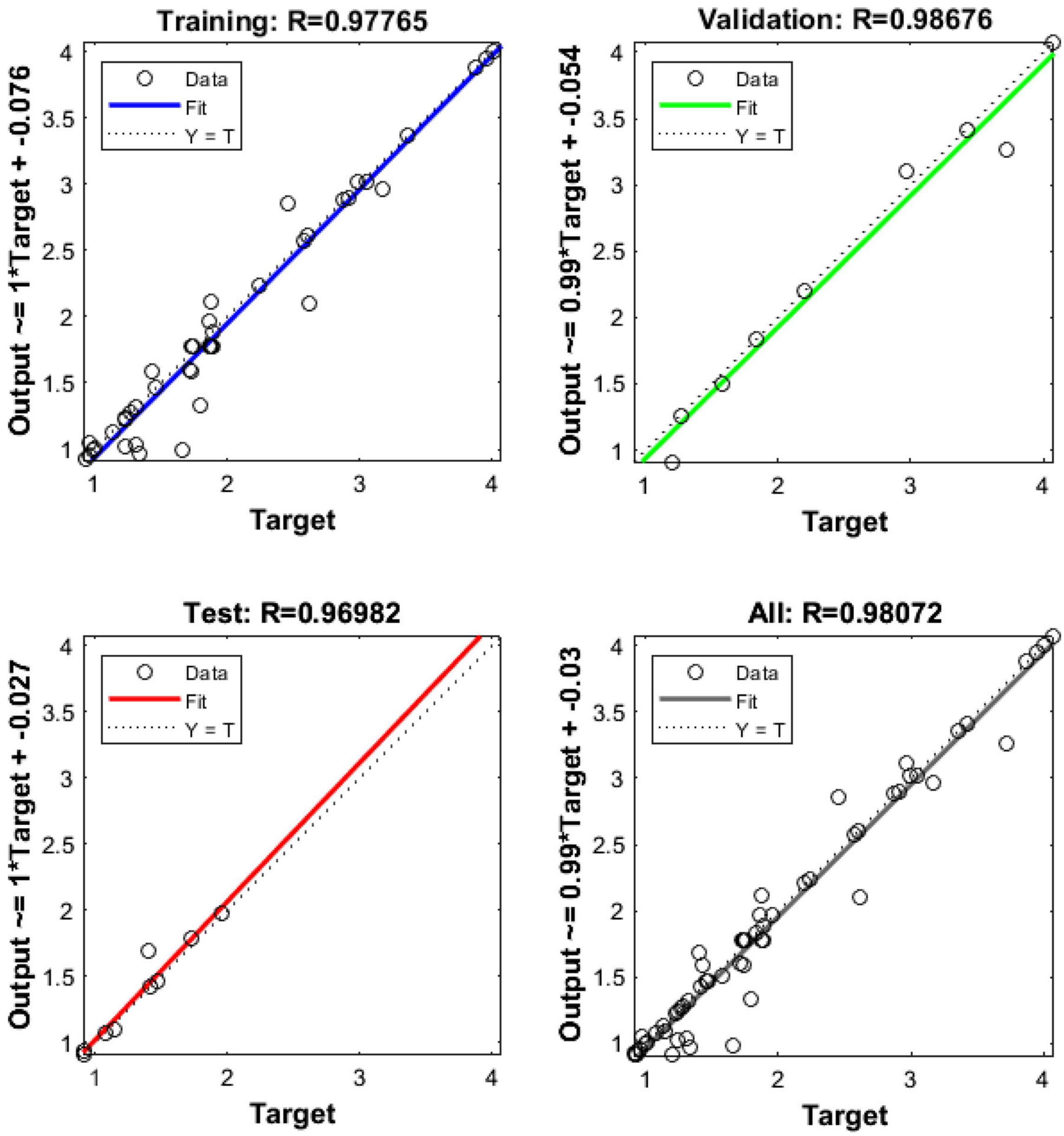

Fig. 6 Linear regression analysis for experimental and estimation made using ANN for Mohamed et al. [16]

5 Accuracy prediction of existing models through ANN

In general, several mathematical modelling techniques have been used for the material extrusion processes. Among these mathematical modelling RSM is commonly used for the prediction and to formulate an expression between process parameters and responses. The accuracy of the fitness model used by the authors is either not significant or prediction is not accurate. Nevertheless, new challenges have to be overcome when predicting the response at various combinations of process parameters. Thus, in this study, to find the consequence of the process variables on the response, first the developed model is used and later it is compared with the ANN model.

In the paper (Mohamed et al. [16]), error percentage in dimension was selected as a response by the authors. Higher the error percentage in the dimension, higher will be error in printed part with respect to 3D digital model. So, for getting the accurate and less error in the part, response taken in this paper should be minimum. The accuracy estimation for the conducted experiments using ANN and RSM have been illustrated in the Fig. 7. From the Fig. 7, it can be concluded that the performance of both models is upright.

In this section, the effect of the process variables is quantified based on the developed RSM and trained ANN

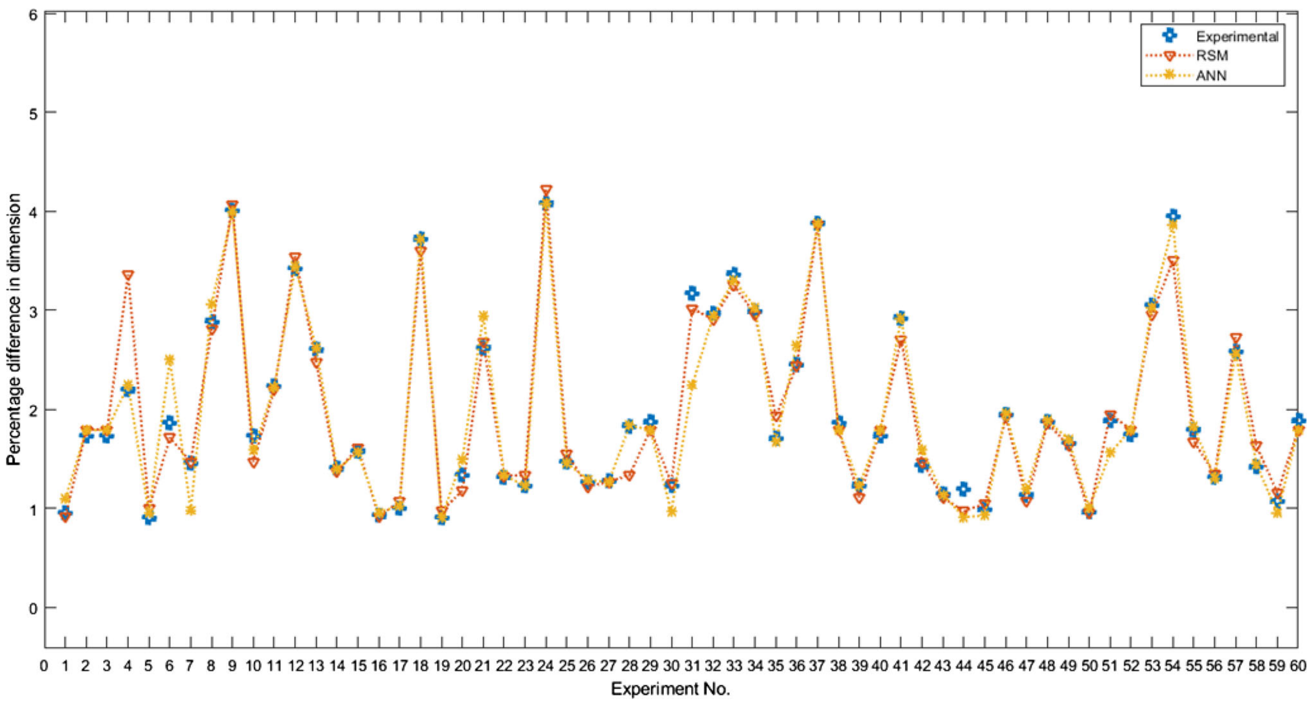

Fig. 7 Comparison plot of RSM and ANN with experimental value

mathematical model. The effect of the considered process variables by the authors on the percentage difference in dimension are shown in Fig. 8 (a) to (f). It is observed from Fig. 8(a) and (f) that on increasing the layer thickness and no. of contours, as can be seen in RSM and ANN models the increment in the error percentage also taking place. In the case of layer thickness, worst dimensional accuracy is obtained at higher layer thickness (i.e., at 0.3302 mm) because higher layer thickness develops voids and internal stress that leads to deformation, it can be observed from microscopic images (Fig. 9). As the air gap increases, there is a prominent increase in dimensional accuracy (Fig. 8e) because when the air gap is small, it restricts heat dissipation rate so that instability generates in the part and leads to permanent deformation up to a certain level of air gap. At the smaller raster angles (upto 45°), a very little change in dimensional accuracy is obtained but further increase in the raster angle dimensional accuracy is enhanced because at larger raster angles shorter lengths of rasters and sharp corners will be deposited in internal part of the specimen. Increasing the angle of build direction, percentage error in dimension first decreases and then increases. At the 0° build orientation part is printed parallel to X-direction (i.e., along part's length), thus long-long rasters are deposited which leads to deflection in the printed part, whereas in case of 90° build orientation, the shorter rasters are deposited which leads to non-uniform temperature distribution. On the basis of analysis of variation performed by the authors and Fig. 8 (a-f) it can be concluded that only layer thickness, raster angle air gap, and number of contours are significant factors while road width and build orientation are insignificant factors.

For the validation of ANN model with the given model, literature by Vyavahare et al. [17] is chosen. In the paper Vyavahare et al. [17] dimensional accuracy of the outer region (i.e., length, width, height, and thickness) as well as inner region (i.e., diameter) of fabricated parts was investigated. The CAD 3D model and the fabricated parts are shown in Fig. 4.

The error in dimensions was calculated by using the Eq. 2. Figure 10 shows the prediction plot for the percentage dimensional error along length, diameter, width, and height. From the Fig. 10 it can be extracted that the ANN model predicts the response more accurately than the model used in the literature. The main effect plot for each response with respect to considered process variables (layer height, printing speed, road width, build orientation, and print temperature) is collectively shown in the Fig. 11. To find the deviation in responses at a single set of variables one experiment was repeated for 5 times. By repeating the experiments, there is 0.5% fluctuation in the response is observed. So, if the process variable does not change the responses more than the 0.5% then it is considered as a dead process variable. Figure 11 (a) to (d) show the variation of the percentage error in length, width, diameter, and height with process variables based on the existing mathematical modelling equation and proposed ANN model. From the Fig. 11 (a-d) it can be observed that layer thickness is a significant factor for all the responses. Print speed is an insignificant factor for the percentage error along width,

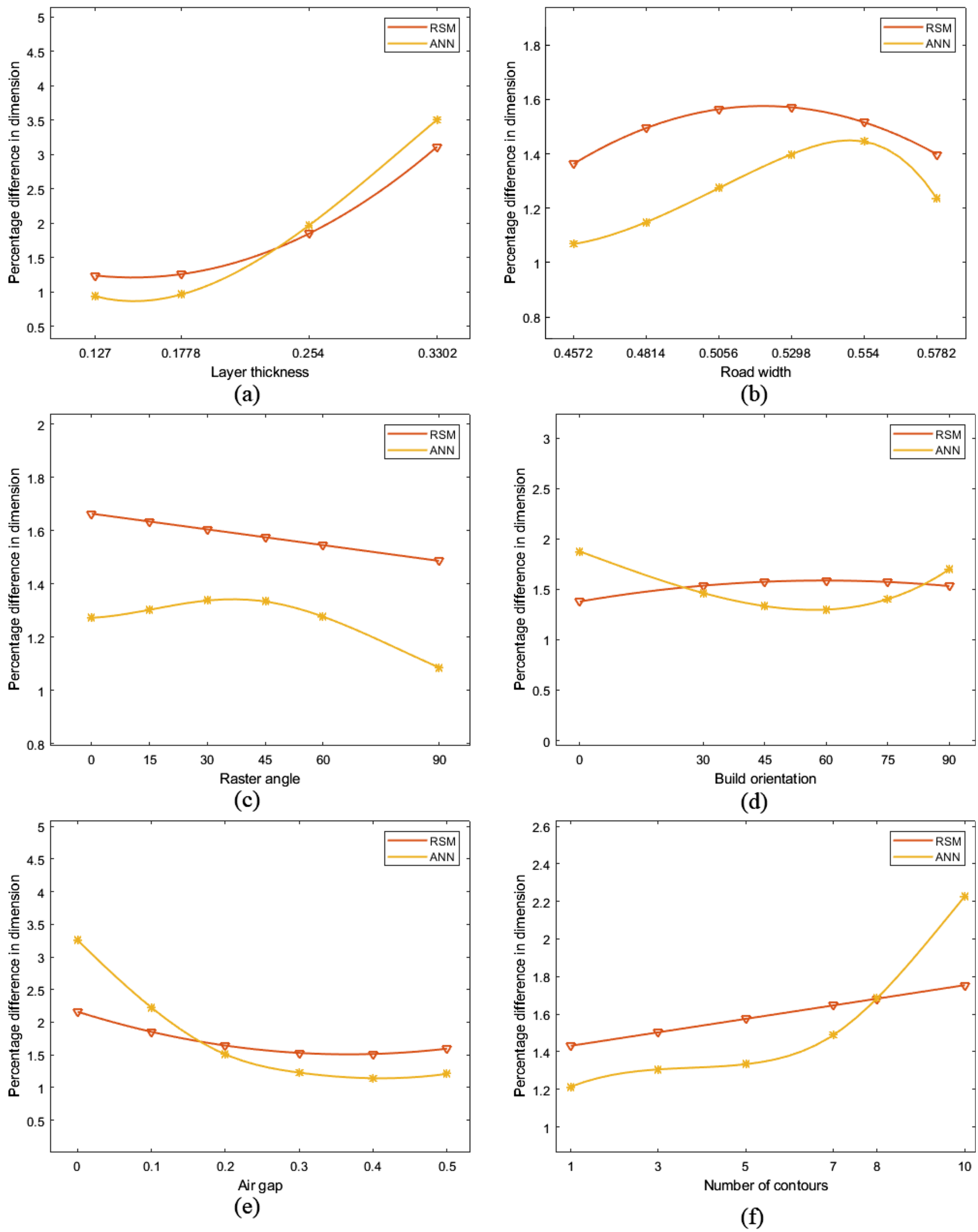

Fig. 8 Variation of percentage difference in dimension as per RSM and ANN model with respect to (**a**) Layer height, **b** road width, **c** raster angle, **d** build orientation, **e** air gap and **f** no. of contours

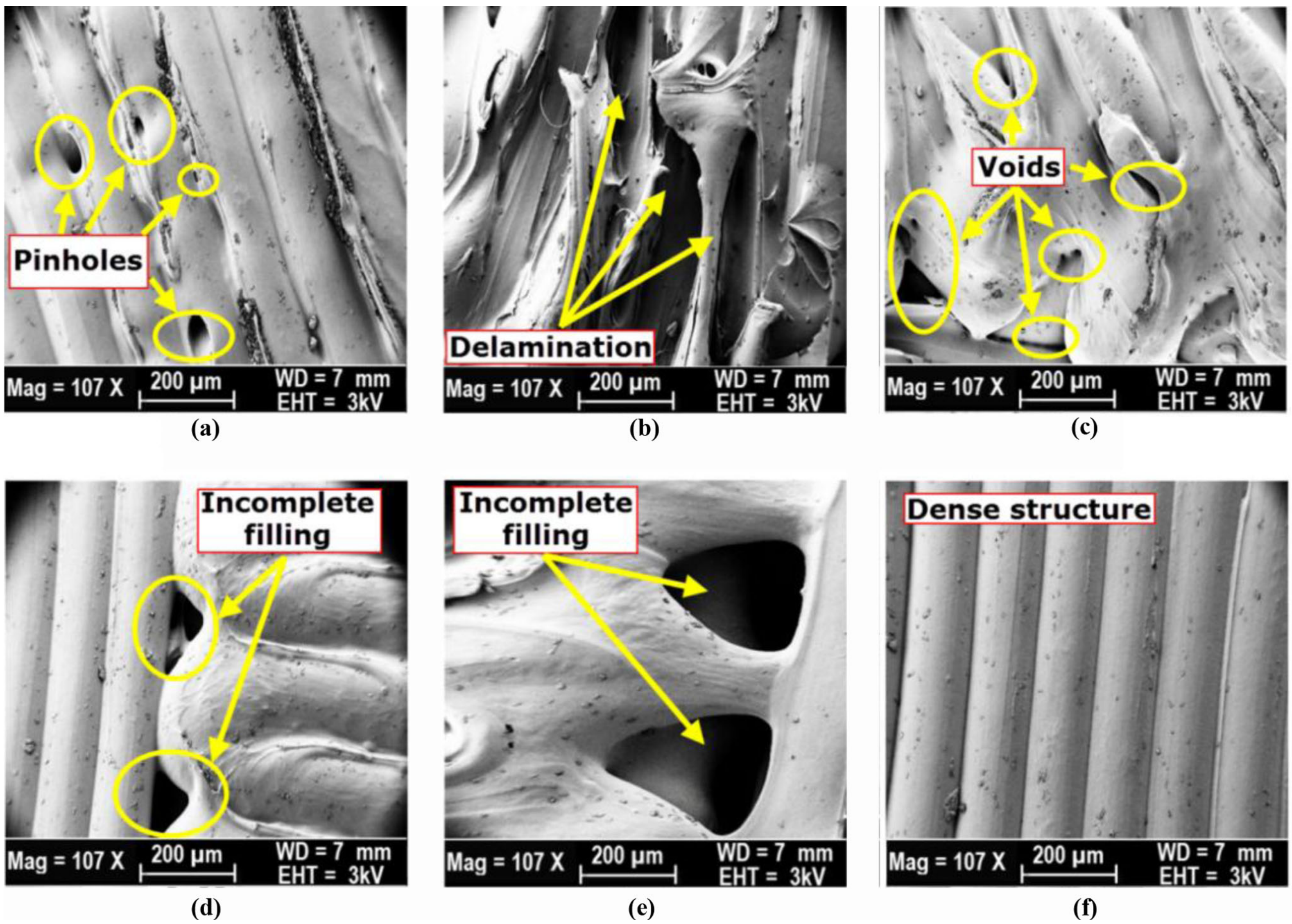

Fig. 9 Scanning electron microscopic images of various parts [16]

length, and diameter but it contributes significantly to dimension along height. Orientation is not a significant factor for the dimension along length and width while it affects the dimension along diameter and height. Wall thickness is the only parameter which has a significant effect on all the responses measured. Extrusion temperature is an insignificant factor for the percentage error along length, width but it can be considered as a significant factor for the percentage error along diameter and height. It is clear from the Fig. 11 that approximate estimation using RSM is quite same, but ANN prediction is much closer to experimental results.

In the paper Jung et al. [18] discharge time is measured by varying the outlet size (i.e., nozzle diameter) and hopper angle. Three cases are considered for different pellet sizes. In the first case 100% pellets are of the size of 12 mm diameter, in the second of 50% pellets are of 12 mm in diameter and 50% are 20 mm diameter and in the third case 100% pellets are of 20 mm diameters. Discharge time is an important factor which affects dimensional accuracy. If discharge is lower or higher than the desired value, then the lack of flow or overflow may occur which leads to instability in the dimensional accuracy. For the prediction of response (i.e., discharge time) given mathematics is compared with the ANN. Figure 12 shows the prediction of the response for all three cases. From the Fig. 12 it is clearly visible that ANN prediction is more accurate than the RSM model prediction. The variation of discharge time with respect to the size of outlet and hopper angle, has been shown in Fig. 13. In each case as the values of both process variables increases discharge time decreases according to both models. But the only difference in both prediction models are the types of curves. In the case of RSM prediction mostly responses vary linearly while in ANN prediction responses vary in quadratic manner. The decrease in the discharge time with the increase in hopper angle is because pressure generation is lower at greater hopper angle. Also, discharge time decreases with outlet size because as the outlet size increases the area of the nozzle increases, so that lesser velocity of flow (i.e., low flow rate) is obtained.

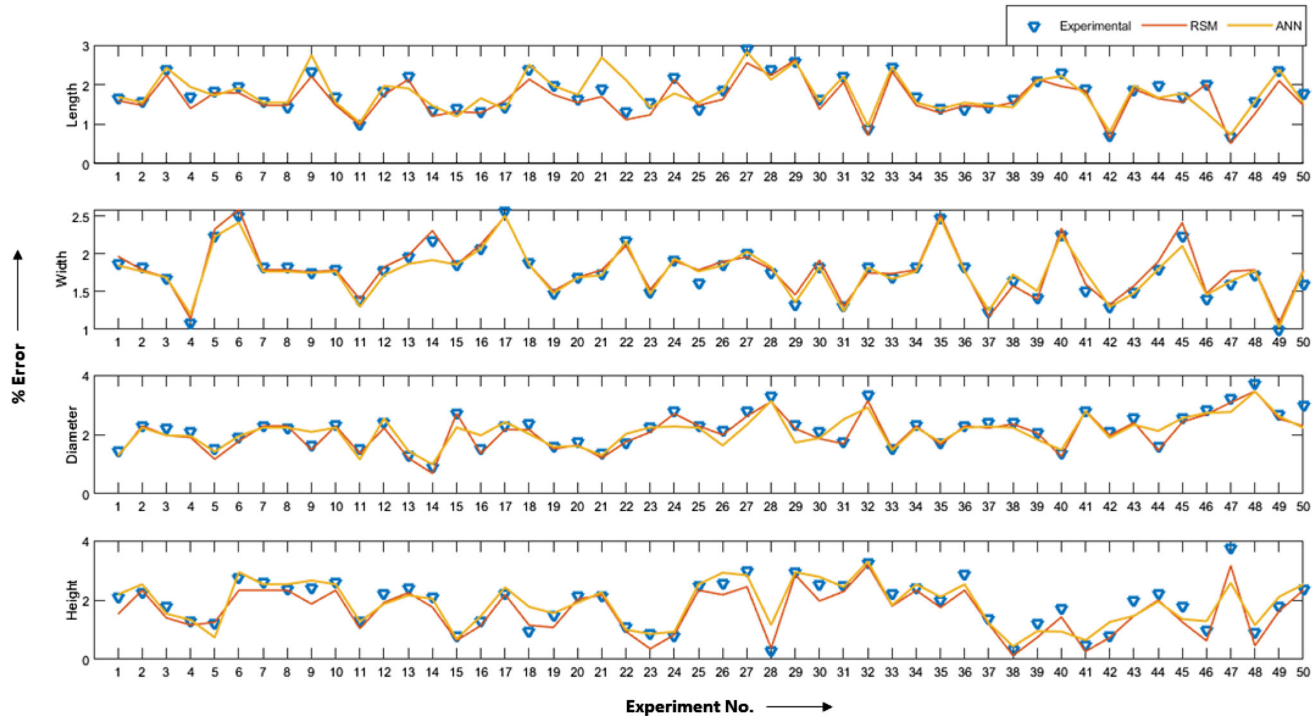

Fig. 10 Comparison plot of RSM and ANN with experimental value

5.1 Root mean square error (RMSE)

RMSE provides data on short-term efficiency, which is defined as the difference between actual and predicted values. The lower the RMSE, the more precise the assessment. The RMSE value for the performed analysis is calculated using Eq. 13 [24].

$$RMSE = \sqrt{\frac{1}{N}\sum_{i=1}^{N}\left(\left(X_i^{actual} - X_i^{predicted}\right)^2\right)} \tag{13}$$

The lesser average RMSE for the developed ANN indicates that it has better performance than the models available in the literature. As shown in Fig. 14, the implemented ANN network can predict a lower average error value of 0.49, under the conditions such as materials, machines and processing conditions. While the average error estimated by existing models is higher even in the literature. These models are only useful for a limited set of process parameters, materials, and machines. Above discussion validate that the developed ANN model can estimate accurate results under random situations, which also ensure the robustness of the developed model.

6 Conclusion and future scope

Part dimensional accuracy in the extrusion-based AM processes is the one of the major factors to decide part quality. To enhance the dimensional accuracy of the components fabricated by fused filament fabrication and screw-based pellet extrusion processes, mathematical modelling of the percentage difference on the dimension is applied. Previously available empirical modelling is not sufficient to predict dimensional accuracy. Therefore, in this study the experimental data has been extracted from the existing literature and ANN techniques is implemented on it. Following outcomes is obtained from the presented study.

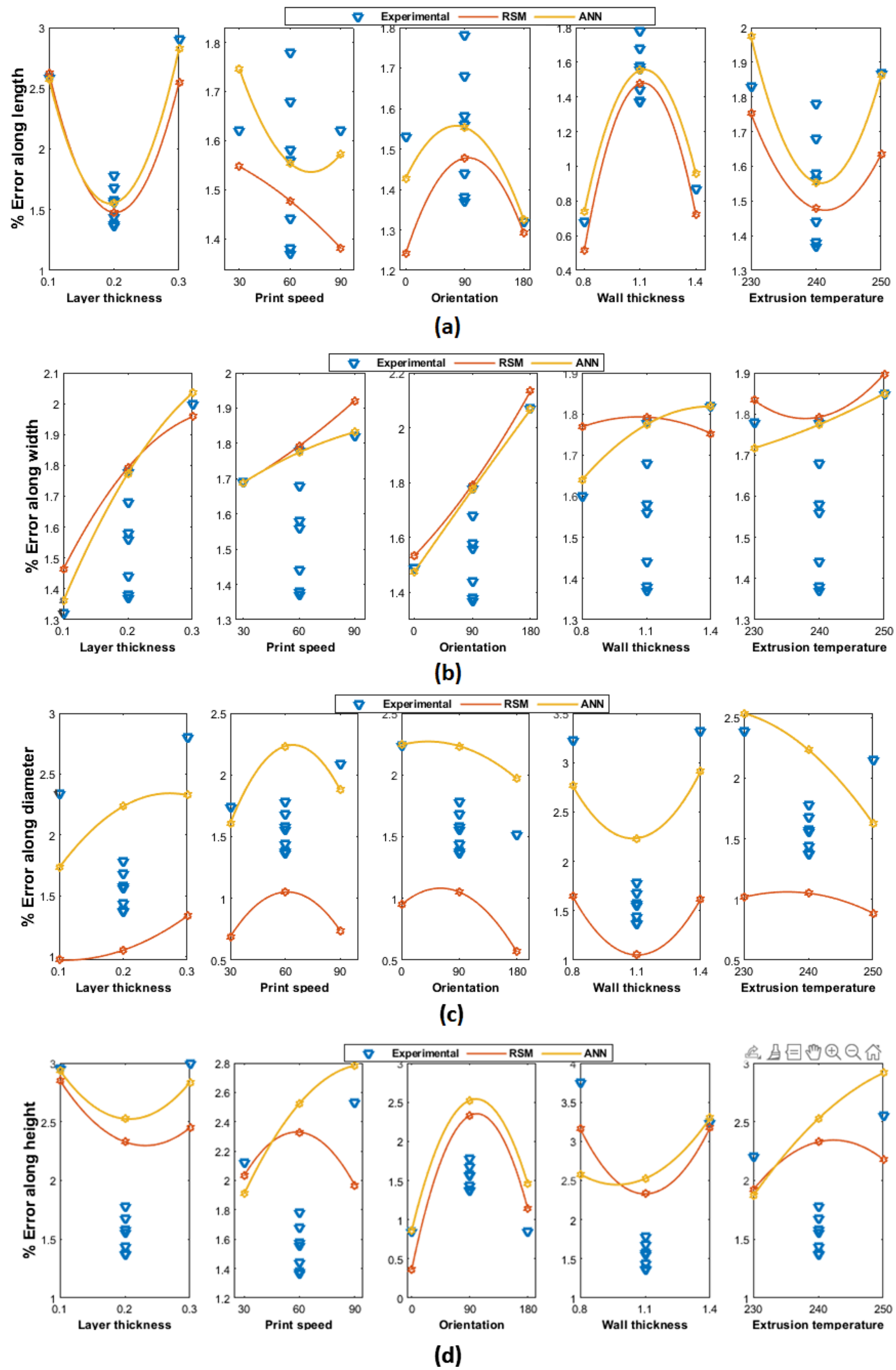

Fig. 11 Effect of process variables (**a**) on diemnsional percentage error in length (**b**) on dimensional error percentage in width (**c**) dimesnional error percentage in diameter (d) on percentage difference in height

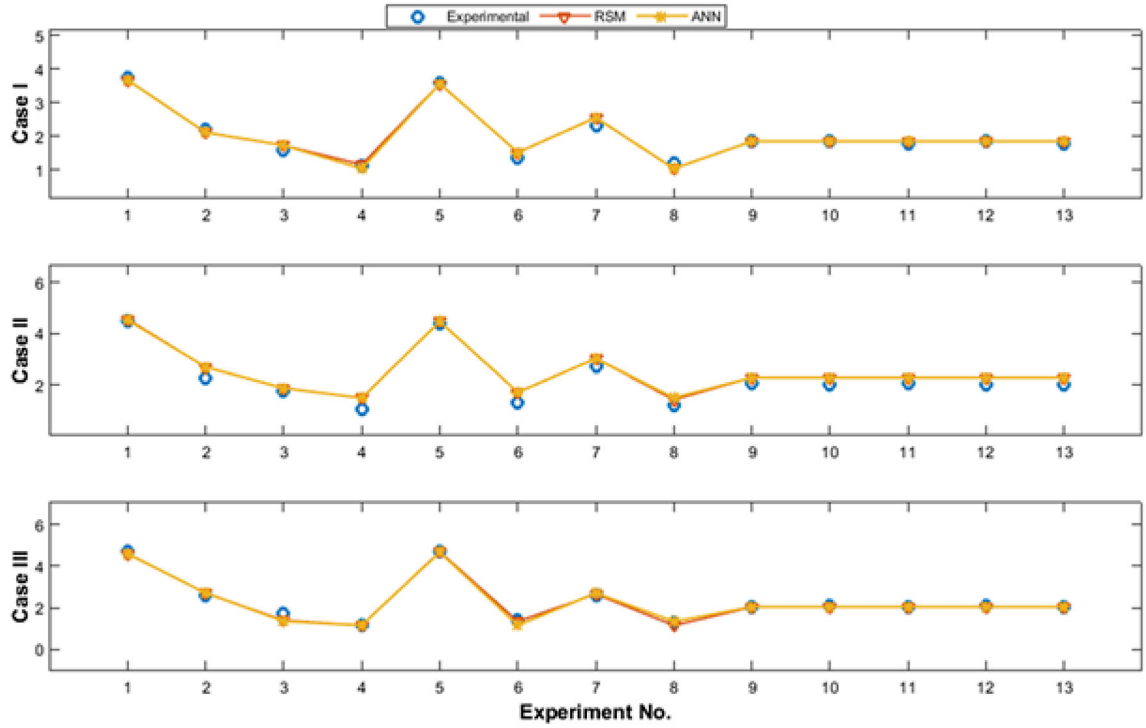

Fig. 12 Comparison plot of RSM and ANN with experimental value

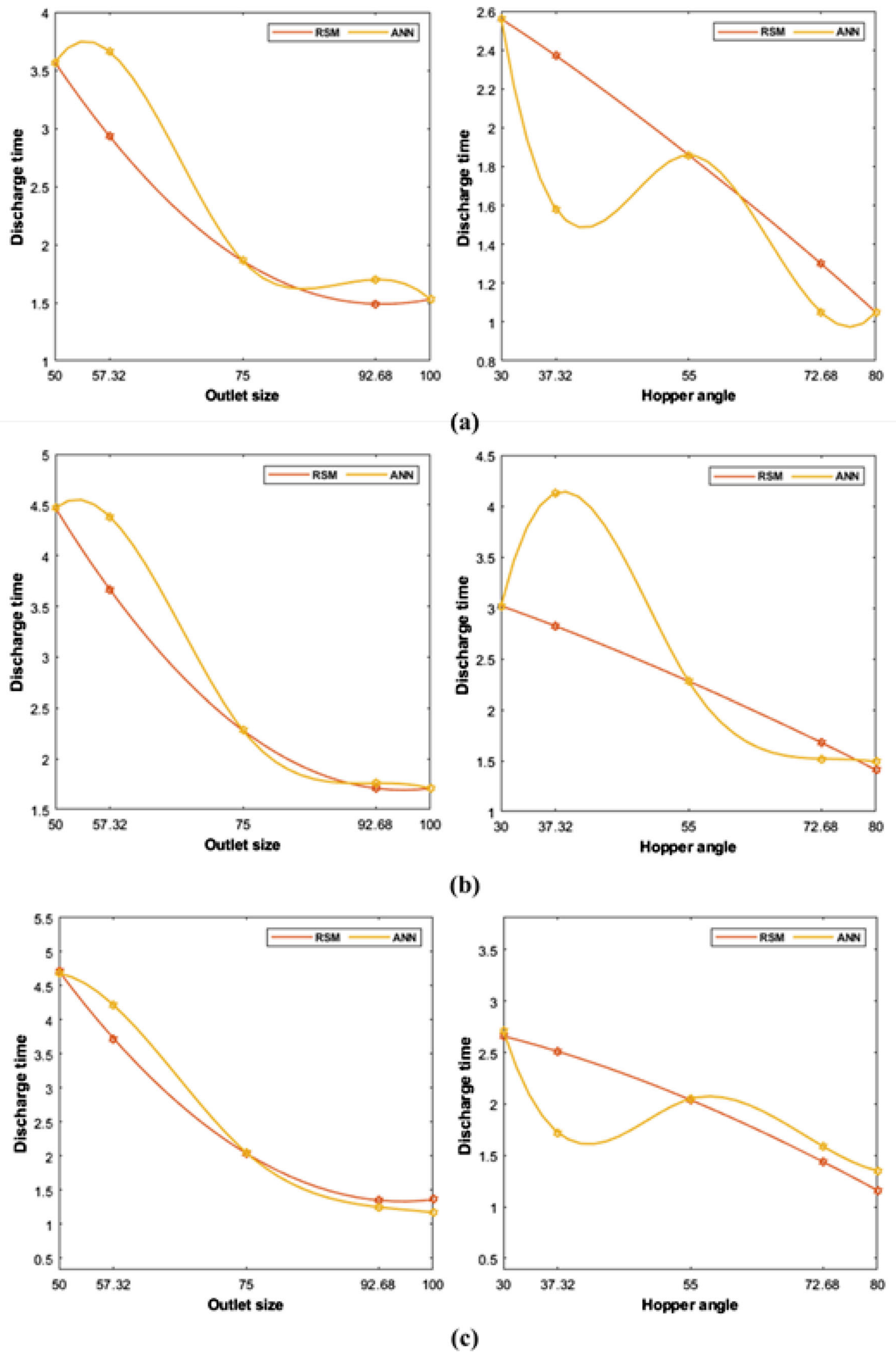

Fig. 13 Effect of process variables on discharge time

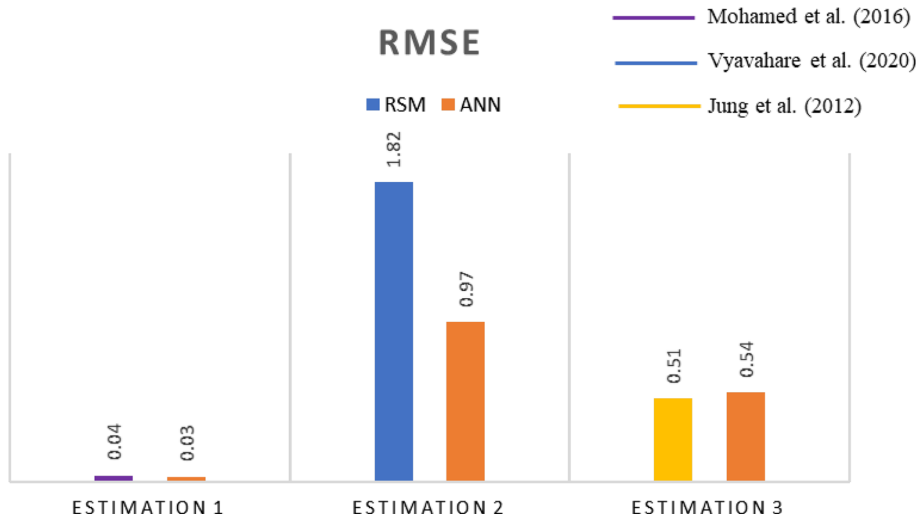

Fig. 14 Comparision plot of RMSE for the RSM and ANN

- The ANN estimation accuracy is dependent on the ANN variables, therefore, to ensure better performance, the formulated model has been trained several times.
- The precision in most of the experiments is about 0.5% of average value. Thus, only that parameter is needed to be studied which changes the dimension greater or lower than the value obtained at the previous level of that parameter.
- The sum of RMSE for RSM and ANN model is 2.27 and 1.54 respectively. So, the estimation of ANN is more acceptable than the existing used model.
- Although ANN is time taking technique, hence it should be used for large data set and more accuracy. The presented study states that RSM and ANN are suitable for optimization of MEAM process. It is also helpful to eliminate complications and a large number of experimental trials.

Despite improving the proposed model's dimensional accuracy, future directions of this work could include investigating the tensile behavior, compression behavior, buckling behavior, and failure mechanism of material extrusion additive manufactured thermoplastic polymer parts using finite element analysis.

Acknowledgements This work was supported by the Science and Engineering Research Board (SERB) – DST under its Start-up Research Grant (SRG) scheme [Grant Number: SRG/2019/000943]

Declarations

Conflict of interest The authors declare that they have no known competing financial interests or personal relationships that could have appeared to influence the work reported in this paper.

References

1. Kumar, N., Jain, P.K., Tandon, P., Pandey, P.M.: Investigation on the effects of process parameters in CNC assisted pellet based fused layer modeling process. J. Manuf. Process. **35**, 428–436 (2018). https://doi.org/10.1016/j.jmapro.2018.08.029
2. Gupta, A.K., Taufik, M.: Effect of process variables on performances measured in filament and pellet based extrusion process. Mater. Today Proc. **47**, 5177–5184 (2021). https://doi.org/10.1016/j.matpr.2021.05.508
3. Dizon, J.R.C., Espera, A.H., Chen, Q., Advincula, R.C.: Mechanical characterization of 3D-printed polymers. Addit. Manuf. **20**, 44–67 (2018). https://doi.org/10.1016/j.addma.2017.12.002
4. Gupta, A.K., Taufik, M.: The effect of process parameters in material extrusion processes on the part surface quality: a review. Mater. Today Proc. **50**, 1234–1242 (2022). https://doi.org/10.1016/j.matpr.2021.08.110
5. Budzik, G., Woźniak, J., Paszkiewicz, A., Przeszłowski, Ł, Dziubek, T., Dębski, M.: Methodology for the quality control process of additive manufacturing products made of polymer materials. Materials (2021). https://doi.org/10.3390/ma14092202
6. Chen, J., Smith, D.E.: Filament rheological characterization for fused filament fabrication additive manufacturing: a low-cost approach. Addit. Manuf. (2021). https://doi.org/10.1016/j.addma.2021.102208
7. Nieto, D.M., López, V.C., Molina, S.I.: Large-format polymeric pellet-based additive manufacturing for the naval industry. Addit. Manuf. **23**, 79–85 (2018). https://doi.org/10.1016/j.addma.2018.07.012
8. Mohamed, O.A., Masood, S.H., Bhowmik, J.L.: Modeling, analysis, and optimization of dimensional accuracy of FDM-fabricated parts using definitive screening design and deep learning feedforward artificial neural network. Adv. Manuf. **9**(1), 115–129 (2021). https://doi.org/10.1007/s40436-020-00336-9
9. Garg, A., Bhattacharya, A., Batish, A.: on surface finish and dimensional accuracy of FDM parts after cold vapor treatment. Mater. Manuf. Processes **31**(4), 522–529 (2016). https://doi.org/10.1080/10426914.2015.1070425
10. Oliveira, T.T., Reis, A.C.: Fabrication of dental implants by the additive manufacturing method: a systematic review. J. Prosthet. Dent. **122**(3), 270–274 (2019). https://doi.org/10.1016/j.prosdent.2019.01.018

11. Pérez, C.J.L.: Analysis of the surface roughness and dimensional accuracy capability of fused deposition modelling processes. Int. J. Product. Res. (2010). https://doi.org/10.1080/00207540210146099
12. Zhang, Y., Chou, Y.K.: Three-dimensional finite element analysis simulations of the fused deposition modelling process. Proc. Inst. Mech. Eng. Part B J. Eng. Manuf. **220**, 1663–1672 (2006). https://doi.org/10.1243/09544054JEM572
13. Salmi, M., Paloheimo, K.S., Tuomi, J., Wolff, J., Mäkitie, A.: Accuracy of medical models made by additive manufacturing (rapid manufacturing). J. Cranio-Maxillofac. Surg. **41**(7), 603–609 (2013). https://doi.org/10.1016/j.jcms.2012.11.041
14. "Cranial Implants – AIP SCIENTIFIC." https://aipsci.com/cranial-implants/ (accessed Sept. 08, 2022)
15. Thompson, M.K., et al.: Design for additive manufacturing: trends, opportunities, considerations, and constraints. CIRP Ann. Manuf. Technol. **65**(2), 737–760 (2016). https://doi.org/10.1016/j.cirp.2016.05.004
16. Mohamed, O.A., Masood, S.H.: Experimental investigation for dynamic stiffness and dimensional accuracy of FDM manufactured part using IV-Optimal response surface design. Rapid Prototyp. J. **4**, 736–749 (2017). https://doi.org/10.1108/RPJ-10-2015-0137
17. Vyavahare, S., Kumar, S.: Experimental study of surface roughness, dimensional accuracy and time of fabrication of parts produced by fused deposition modelling. Rapid Prototyp. J. **9**, 1535–1554 (2020). https://doi.org/10.1108/RPJ-12-2019-0315
18. Jung, U., An, J., Lim, B., Koh, B.: Modeling discharge of pellets from a hopper using response surface methodology. Int. J. Precis. Eng. Manuf. **13**(4), 565–571 (2012). https://doi.org/10.1007/s12541-012-0072-9
19. Singh, R.P., Kumar, N., Gupta, A.K., Painuly, M.: Investigation into rotary mode ultrasonic drilling of bioceramic: an experimental study with PSO-TLBO based evolutionary optimization. World J. Eng. **19**, 274 (2021). https://doi.org/10.1108/WJE-03-2021-0179
20. Lee, S.H., Park, W.S., Cho, H.S., Zhang, W., Leu, M.C.: A neural network approach to the modelling and analysis of stereolithography processes. Proc. Inst. Mech. Eng. B J. Eng. Manuf. **215**(12), 1719–1733 (2001). https://doi.org/10.1177/095440540121501206
21. Mahmood, M.A., Visan, A.I., Ristoscu, C., Mihailescu, I.N.: Artificial neural network algorithms for 3D printing. Materials **14**(1), 163 (2021). https://doi.org/10.3390/ma14010163
22. Kataria, R., Singh, R.P., Alkawaz, M.H., Jha, K.: Optimization and neural modelling of infiltration rate in ultrasonic machining. OPSEARCH **59**(1), 146–165 (2022). https://doi.org/10.1007/S12597-021-00534-4
23. Moradi, M.J., Khaleghi, M., Salimi, J., Farhangi, V., Ramezanianpour, A.M.: Predicting the compressive strength of concrete containing metakaolin with different properties using ANN. Measurement **183**, 109790 (2021). https://doi.org/10.1016/j.measurement.2021.109790
24. Gupta, A.K., Taufik, M.: Improvement of part strength prediction modelling by artificial neural networks for filament and pellet based additively manufactured parts. Aust. J. Mech. Eng. **00**(00), 1–18 (2022). https://doi.org/10.1080/14484846.2022.2047472